https://doi.org/10.15407/ujpe71.4.392

N.I. OSTAPENKO,[1] V.I. SUGAKOV[2]

[1] Photoaktivity Department, Institute of Physics of the Nat. Acad. of Sci. of Ukraine
(46, Prosp. Nauki, 46, Kyiv 030680; e-mail: nina.ostapenko@gmail.com)
[2] Institute for Nuclear Research of the Nat. Acad. of Sci. of Ukraine
(47, Prosp. Nauki, Kyiv 03680; e-mail: sugakov@kinr@kyiv.ua)

FEATURES OF MOLECULAR VIBRATIONAL EFFECTS ON POLYMER THERMOLUMINESCENCE

The paper presents the results of observation and investigation of the manifestations of individual molecular vibrations in polymer thermoluminescence processes. The features of these manifestations are as follows: 1) despite the quasi-continuous spectrum of trap energies for charge carriers in polymers, the activation energies, determined by fractional thermoluminescence method, exhibit discrete values; 2) these activation energy values coincide with the quanta of molecular vibrations in the system; 3) the temperature dependence of the thermoluminescence intensity reveals specific features caused by molecular vibrations. This temperature dependence, and the activation energies were experimentally investigated for polymers deposited on different substrates, polymers with varying degrees of crystallinity, and nanoscale polymer systems embedded in porous silica. The experimental results are consistent with the proposed model of the participation of molecular vibrations in the processes of charge release from traps during thermoluminescence.

K e y w o r d s: thermoluminescence, polymer films, nanocomposites, molecular vibrations, activation energies.

1. Introduction

M.T. Shpak made a major contribution to the study of the optics of molecular crystals and laser processes [1, 2]. In recent years, he also began actively studying the optical properties of polymers [3]. In this paper, we present the results of studies concerning one of the mechanisms of thermally stimulated luminescence (TSL), studied by us experimentally and theoretically for polymers (both films and nanocomposites). During TSL external action (for example, optical irradiation) causes charge separation, created electrons and holes are captured by traps and become separated in space. This state is excited. When the system is heated, charges can overcome the energy barrier located between charges and recombine, emitting the TSL light. Overcoming the barrier, called the activation energy, is one of the important processes in TSL. The activation energy determined from the TSL data provides important information about the state of the traps in the system. Overcoming the barrier in TSL occurs with the participation of many vibration states. However, in our work using the example of silicon organic polymers, we have observed that processes are possible with the participation of one or several optical vibrations, which lead to the appearance of features in the TSL curve and the observation of discrete activation energies of trap levels by the fractional TSL method, although the spectrum of trap levels in polymers is quasi-continuous.

The influence of molecular motions in polymers on the manifestation of TSL and thermally stimulated conductivity has been noted by many authors for a long time [4–11] in pure polymers, in polymers with introduced impurities and irradiated with radiation or electrons. The authors note the following circumstances: 1) the activation energy is determined primarily by the structure and properties of the original polymer [5, 8, 10], 2) there is a closeness of the

C i t a t i o n: Ostapenko N.I., Sugakov V.I. Features of molecular vibrational effects on polymer thermoluminescence. *Ukr. J. Phys.* **71**, No. 4, 392 (2026). https://doi.org/10.15407/ujpe71.4.392.

activation energies of TSL and relaxation processes in the polymer [5, 7, 8, 10], 3) in the work of Gorban *et al.* [12], a coincidence of the activation energy measured using the fractional TSL method and the energy of the vibration quantum obtained from the Raman spectra in inorganic crystals was observed experimentally. A similar coincidence was observed in the several subsequent works (see the references in [13]) in many inorganic materials (NaCl, KCl, Al_2O_3 and others). Using traditional approaches to determine the spectra of electron levels from activation energy data, the authors of these works came to contradictory results: the appearance of discrete trap levels in the crystal, although there are no interactions for such a conclusion. Activation energies that coincide in magnitude with the photon energies were also observed in polymers [14, 15], which, with the traditional approach, should be interpreted as the presence of discrete electron levels in the polymer, although the electron spectrum in such traps in a disordered system such as a polymer is continuous.

To explain the coincidence of activation energies and vibration quanta and other above-mentioned features of TSL, the authors of work [16] proposed a mechanism according to which the coincidence is observed due to the process in which the charge is detached from the trap and transferred to the recombination center due to the absorption of separate molecular vibration. Thus, individual vibrations stimulate TSL processes. In this process, the activation energy (a shelf in the fractional TSL method) is a molecular vibration energy necessary for the charge to escape from the trap to the region of conductive states. Here and hereafter, by the word "region" we mean not a spatial area, but a region of energies in the polymer in which the movement of charge and its recombination with the emission of light occur. With such a mechanism, the traps take part, whose levels are removed from the conducting states by the value of the energy of the quantum of vibrations. This means that the activation energy E_α must be equal to the energy of the vibrational quantum $E_\alpha = \hbar\omega$. Also, since the activation energy is determined by the energy of the quantum of vibrations, it must depend on the polymer, and not on the method of creating the defect, which is observed for many bands. According to work [16], the model predicts the appearance of a structure on the TSL curve, which was experimentally detected in various polymers [16–19].

2. Model Consideration of the Effect

The process of TSL consists of several stages: 1) the transfer of the charge state from a localized state to the conductive states of polymer, 2) the charge recombination with a charge of the opposite sign, 3) the photon emission by an excited state or energy transfer to vibrational states. In our works, during the theoretical consideration of the problem, the initial stage was studied, that is the jump of the charge from the localized state to the conductive states, under the assumption that the radiation intensity during TSL should be proportional to the probability of such a jump.

In theoretical part of the work, the kinetics of the charge transfer from localized to conductive states is investigated. We consider a polymer, in which an external irradiation creates charge carriers of opposite signs localized (trapped) at different spatial points throughout the material. We also assume that the charges of a certain sign (for example, electrons) are localized on deeper levels and, therefore, for the study of TSL, it is enough to consider the release from traps of carriers of only one type (for example, holes). If the energy of the released charges is in the region of conductive states, then, moving across the polymer, they can recombine with the charges of the opposite sign, emitting photons. Also, we suppose that the concentration of the carriers is not large and the different pairs of the charges of opposite sign (geminate pairs), created by independent photons are localized far apart, i.e. the distance between the geminate pairs is much larger than the distance between the charges of a single pair.

With increasing temperature the probability of the carrier's transition from the trap to the conductive region consists of the sum of the separate probabilities of such transitions assisted by different vibrations. We assume, that the probability of the transition induced by one or several vibrations with the frequency ω_α exceeds the probabilities assisted by other vibrations. It is precisely this vibration that leads to a formation of the fine structure in TSL. Thus, in the kinetic equation for the density of localized carriers, the term, which describes the transitions caused by these particular vibration modes, will be written separately. Let us denote the carrier density distribution by $n(E,t)$, where E is the energy of the localized state relative to conductive states (for example, it co-

incides with the transport energy), thus E assumes a negative value. The change of the density per unit time is proportional to the density multiplied by the probability of the transition from the localized state to the conductive states. (We neglect inverse transitions). Therefore, the following equation must be solved in order to determine the time dependence of the distribution of the carriers' density

$$\frac{dn\,(E,t)}{d\,t} = -n\,(E,t)\Bigg(\sum_{\alpha} P_{\alpha}(E,\hbar\omega_{\alpha},T) + \\ + P\,(E,T)\,\exp(-\,|E|\,/\kappa T)\Bigg), \tag{1}$$

where α denotes the numbers of the most active vibration modes in TL, $P_{\alpha}(E,\hbar\omega_{\alpha},T)$ is the probability of transition of a charge with energy E to the conductive region due to absorption of vibration of the type α with energy $\hbar\omega_{\alpha}$. The second term in the parenthesis of the right-hand side α of equation (1) describes all other transitions to the conductive region including multiphonon ones [20], $P\,(E,T)$ is equivalent to the attempt-to-jump frequency in the classical theory, the factor $\exp(-|E|/\kappa T)$ describes the temperature dependence of the probability of transitions to higher levels according to the Arrhenius law. The value $P\,(E,T)$ will be considered as a constant parameter of the system when performing specific calculations. It is assumed that the temperature when measuring TL changes according to a linear law $T = T_0 + b(t - t_0)$, where T_0 is the temperature at the start of measurements t_0, b is the heating rate.

Immediately after the irradiation of the system with light, the processes of recombination of charges of opposite signs occur. Only those charges with opposite signs remain in the system, which are located far apart, and the recombination time between them is large. The dynamics of the time evolution of the charge density distribution starting from the nonequilibrium state is presented in Refs. [21–23]. After some initial time at low temperature, the carrier's density distribution changes very slowly. It will be described by charge density distribution of by a Gaussian function

$$n_0(E) = \frac{Nc}{s\sqrt{2\pi}} e^{(-(E-E_d)^2/2s^2)}, \tag{2}$$

where E_d and s are the position of the maximum and the width of the carrier density distribution, Nc is the concentration of the charges. The energy E is measured from the maximum of the Gaussian distribution in the unirradiated sample.

The intensity of the TSL is determined by the contributions from transitions to conductive states of all carriers with different values of the localization energy. We assume that the contributions to the TSL intensity of various selected modes appear at different temperatures and consider the contribution of a separate α-type mode. Using the solution of the Eq. (1) for the case of α-type mode, assuming a linear time dependence of temperature and the initial condition $T(0) = T_0$, we obtain the following equation for the TSL intensity

$$I(T) = C \int\limits_{-\infty}^{\infty} dE\; n_0(E) \Bigg[P_{\alpha}(E,\hbar\omega_{\alpha},T) + \\ + P(E,T) \exp\left(-\frac{|E|}{\kappa T}\right)\Bigg] \times \\ \times \exp\Bigg\{-\frac{1}{b}\int\limits_{T_0}^{T}\Bigg[P_{\alpha}(E,\hbar\omega_{\alpha},T') + \\ + P(E,T') \exp\left(-\frac{|E|}{\kappa T'}\right)\Bigg]\, dT'\Bigg\}, \tag{3}$$

where C is some constant value.

In our works, we studied the influence of the interaction of a charge with molecular vibrations of polymer on TSL: 1) in the first order of the perturbation theory, using a linear expansion with respect to the displacements of nuclei [16–18], 2) taking into account the resonance energy transfer from the optical vibration to the carrier according to Förster–Dexter formalism [19] and 3) in a model of non-adiabatic transitions in Frank–Condon approximation [24].

In Refs. [16–19] the TSL curve was calculated with the participation of several different molecular vibrations (several α-types), but with the participation of one vibration of a given type. Calculations showed that processes involving separated vibrations give rise to features in the TSL curve consisting of the appearance of a peak and a subsequent dip in the curve. Some calculated TSL curves exhibiting such structures will be presented in the experimental part of the paper.

In the following, we will present the application of the model of nonadiabatic transitions to the study of

the shape of the TSL curve, in the formation of which the absorption of several quanta of molecular vibrations of one type of α is considered [24]. The model was employed for the treatment of different processes connected with the change in the wave function of the nuclear subsystem at electron transitions. It was applied to calculate shapes of the absorption and luminescence bands of impurities [25], to describe electron transitions between different states of molecules (see the review [26]), to study charge transfer between molecules in biological systems [27]. In Refs. [28, 29], the model was used for the determination of the probability of charge jumps between molecules in organic semiconductors. We apply the model to study of TSL processes in polymers. We will consider the probability of a carrier's jump between two molecules i and j, assuming that the energy of the carrier localized on molecule i corresponds to a trap, molecule j is in the region of energies of conductive states (for example in the region of the transport energy). It is also assumed that the Hamiltonian describing nuclei is a quadratic function of their displacements, and the presence of a carrier on a molecule leads to the shift in the potential energy, which is a linear function of coordinates. In the adiabatic approximation, the wave functions of nuclei and the carriers localized on molecules i and j have the form, respectively, $\Psi in = \varphi_i(r,q)\Phi_{in}(q)$ and $\Psi jn' = \varphi_j(r,q)\Phi_{jn'}(q)$, where r designates the coordinate of carrier, q are the normal coordinates of nuclei, $\varphi_{i(j)}(r,q)$ is the wave function of the carrier, when it is localized on the molecule $i(j)$, $\Phi_{in}(q)$ and $\Phi_{jn'}(q)$ are the wave functions of the nucleus subsystem, when the carrier is localized on the molecule i and there are n quanta of molecular vibrations in system and the wave function of the nucleus subsystem with carrier on the molecule j and there are n' quanta of molecular vibrations in the system, respectively. In the Condon approach, the wave function depends weakly on positions of nuclei and the transition of carrier between molecules occurs at fixed positions of nuclei. The matrix element of the transition from the state $|i,n\rangle$ to the state $|j,n'\rangle$ is equal to

$$I_{jn',in} = \int drdq\, \Psi_{jn'}(r,q)\, V(r,q)\, \Psi_{in}(r,q) =$$

$$= \langle n'|J_{ji}(q)|n\rangle \approx J_{ji}\langle n'|n\rangle,$$

where $V(r,q)$ is the energy of the carrier interaction with molecules, J_{ji} is the electronic coupling.

The probability of the transition of the charge carrier from the molecule i to the molecule j in the unit time with the change of the vibrational quantum number from n to n' is determined by the equation

$$W_{jn',jn} = \frac{2\pi}{\hbar} J_{ji}^2 P_n \langle n'|n\rangle^2 \delta(E_{jn'} - E_{in}), \tag{4}$$

where P_n is the temperature dependence of the number of vibrational quanta.

The results of calculation of the matrix elements $\langle n'|n\rangle$ are presented in many papers (see, for example, Refs. [25–28]). The calculation of the matrix elements $\langle n'|n\rangle$ using the oscillator wave functions and averaging over molecules with the energy of electronic levels E_i and over the final states with the energy E_j gives using (4) the probability of the charge transition

$$W_{ji} = \frac{2\pi}{\hbar} I_{ji}^2 \sum_{m_\alpha} \prod_{\alpha} D(T, \hbar\omega_\alpha, g_\alpha^2, m_\alpha) \times$$

$$\times\, \delta(E_j - E_i - m_\alpha \hbar\omega_\alpha), \tag{5}$$

where

$$D(T, \hbar\omega_\alpha, g_\alpha^2, m_\alpha) = \exp\left(-g_\alpha^2 \frac{1+z_\alpha}{1-z_\alpha}\right) \times$$

$$\times \exp\left(\frac{m_\alpha \hbar\omega_\alpha}{2\kappa T}\right) I_{m_\alpha}\left(2g_\alpha^2 \frac{\sqrt{z_\alpha}}{1-z_\alpha}\right), \tag{6}$$

I_m is modified Bessel function, $g_\alpha = \sqrt{M_\alpha \omega_\alpha/(2\hbar)}\, g_\alpha^0$ is constant of carrier-vibration interaction,

$$z_\alpha = \exp\left(-\hbar\omega_\alpha/\kappa T\right), \tag{7}$$

M_α and g_α^o are the reduced mass and the shift of the α-th normal coordinate due to the interaction with the carrier, correspondingly, $m_\alpha = n' - n$, I_{ji}^2 is the mean value of J_{ji}^2.

The summation in Eq. (5) runs over all modes of vibration α and over all possible changes of quantum number m_α (positive and negative). The problem of the calculation of the carrier's jump between molecules using Eq. (4) is complicated because its solution requires knowledge of all vibrational spectra. This problem was solved in the Ref. [29] for several polymers, which consist of a restricted numbers of molecules. The authors calculated the charge transfer rates and the mobilities for some organic semiconductors and showed that the application of the quantum mechanical Eq. (4) for carrier jump and all intramolecular vibrations are important for

these calculations. For determination of TSL curve the problem was solved in the Ref. [24] using the following assumptions. The intramolecular modes are vibration states of molecule. They are discrete high-frequency modes and are considered in an Einstein-type approximation. Spectra of intermolecular modes are complicated and are unknown in detail in disordered systems. But they have low frequencies and may be treated classically. As will be seen, their contribution to TSL may be described by a single parameter. In the work [24] the vibrational states of the systems that determine TSL were divided into three parts: 1) the selected state with a frequency ω_α and the states with a multiple of this frequency $m_\alpha\omega_\alpha$, 2) other intramolecular vibrations that do not give structure to the TSL curve or give structure at a temperature region different from the one studied, and 3) low-frequency vibrations with a frequency satisfying the condition $\hbar\omega_\alpha \ll \kappa T$, such modes may be considered as classical. Marcus considered the motion of all molecular vibrations classically [30]. In our work, vibrations with quantum energies of the order of κT or greater are quantum, and the effects observed and studied in this work are also quantum.

As a result in Ref. [24], the following expression was obtained for probability of transition of a charge with energy E to all states of the conductive region

$$P_\alpha(E,\hbar\omega_\alpha,T) = \frac{2\pi}{\hbar} I_{ji}^2 B_\alpha(T) \times$$
$$\times \sum_m D(T,\hbar\omega_\alpha,g_\alpha^2,m_\alpha) \times$$
$$\times \int \frac{\rho(E')}{\sqrt{2\pi}S(T)} \exp\left[-\frac{(E'-E-m_\alpha\hbar\omega_\alpha)^2}{2S(T)^2}\right] dE', \quad (8)$$

where $\rho(E) = \sum_j \delta(E-E_j)$ is the density of states in the conductive region,

$$S(T) = \left(\sum_{\alpha'} 2g_{\alpha'}^2 \kappa T \hbar\omega_{\alpha'}\right)^{1/2},$$
$$B_\alpha(T) = \prod_{\beta\neq\alpha} D(T,\hbar\omega_\beta,g_\beta^2,0_\beta)$$

is the contribution to the probability of charge transition of intramolecular vibrations with $\beta \neq \alpha$, its value depends weakly on the temperature and has order of unity. In the formula for $S(T)$, the summation over α' occurs over all low-energy intermolecular vibrations. Thus, including low-frequency vibrations leads to a broadening by the value of $S(T)$ and to a shift of levels (it is small and is not shown in Eq. (8)).

From Eqs. (6), (8) in the first order in the interaction constant g_α^2 for probability of processes with absorption of single molecular vibration quant of the type α, we obtain following expression

$$P_\alpha(E,\hbar\omega_\alpha,T) = \frac{2\pi}{\hbar} I_{ji}^2 g_\alpha^2 B_\alpha(T) \times$$
$$\times N(\hbar\omega_\alpha,T)\,\Phi(E,T), \quad (9)$$

where $N(\hbar\omega_\alpha,T)$ is the number of molecular vibrations with frequency ω_α at temperature T

$$N(\hbar\omega_\alpha,T) = 1/(\exp(\hbar\omega_\alpha/\kappa T)-1), \quad (10)$$

$$\Phi(E,T) = \frac{1}{\sqrt{2\pi}S(T)} \int dE' \times$$
$$\times \exp\left(-(E'-E-\hbar\omega_\alpha)/(2S(T)^2)\right) \rho(E'). \quad (11)$$

It can be seen that the probability of the transition is proportional to the quantum number of molecular vibrations of the type α. At low temperatures, the structures are observed in the TSL curve, if the frequency of vibrations satisfies the condition $\hbar\omega_\alpha \gg \kappa T$. Therefore, the expression $N(\hbar\omega_\alpha,T) = \exp(-\hbar\omega_\alpha/\kappa T)$ holds, i.e. the temperature dependence of the population of vibrational levels coincides with the population of impurity and defect levels for which the activation energy is equal to the energy of the quantum of molecular vibrations. Thus, the molecular vibrations give the effect in the TSL similar to the effect of defects.

If the broadening of transition $S(T)$ is less than the width of the conductive region ρ_o, the probability of the charge transition given by Eq. (9) for processes with absorption of a single molecular vibration has form

$$P_\alpha(E,\hbar\omega_\alpha,T) = W_\alpha N(\hbar\omega_\alpha,T)\theta(E+\hbar\omega_\alpha), \quad (12)$$

where

$$W_\alpha = w_\alpha g_\alpha^2 \theta(E+\hbar\omega_\alpha),$$
$$w_\alpha = W_\alpha/g_\alpha^2 = \frac{2\pi}{\hbar} I_{ji}^2 B_\alpha(T)\rho_o, \quad (13)$$

$\theta(x) = 1$ at $x \leq 0$ and $\theta(x) = 0$ at $x < 0$.

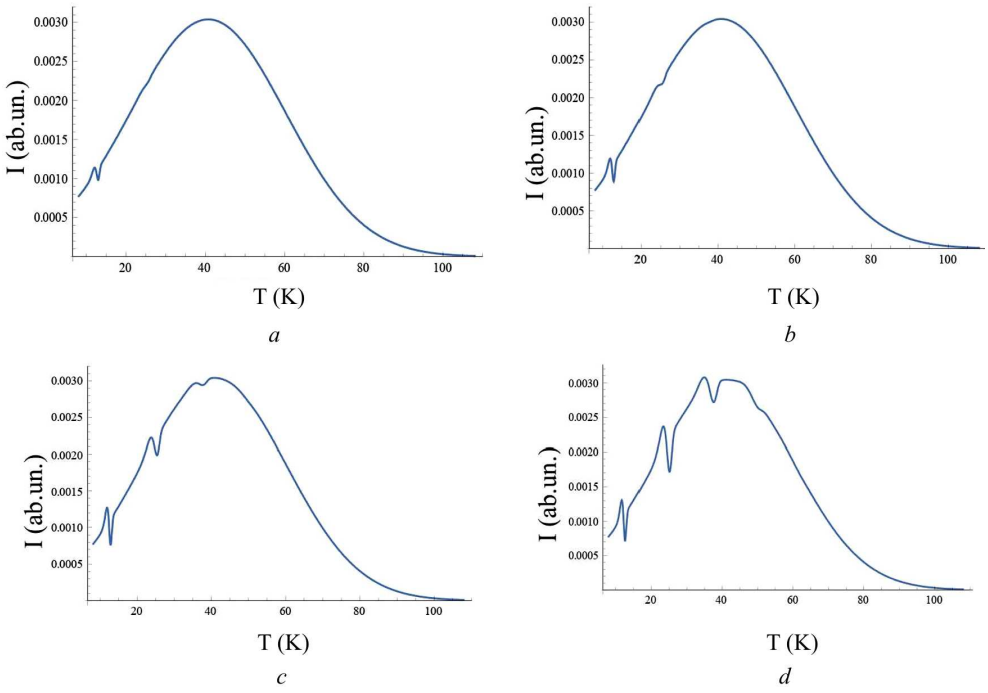

Fig. 1. Calculated TSL curves at $E_d = 0.1$ eV, $s = 0.05$, $\hbar\omega_\alpha = 0.03$ eV, $w_\alpha = 10^{12}$ s^{-1}, $P_\alpha = 10^{11}$ s^{-1} for different values of g_α^2: 0.1 (*a*), 0.2 (*b*), 0.5 (*c*), 1 (*d*)

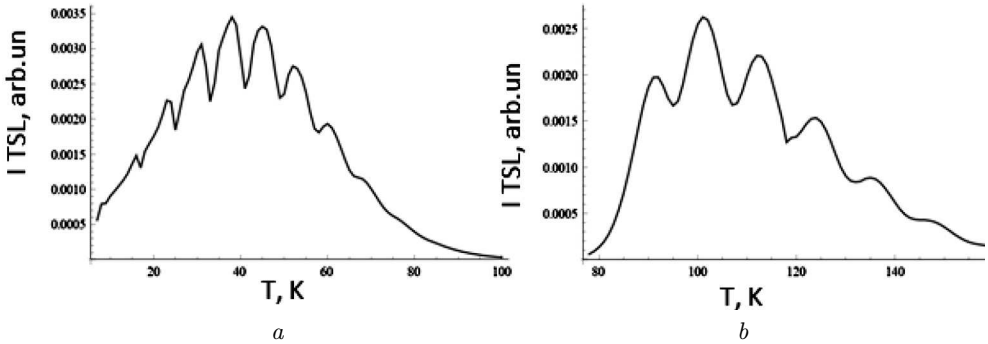

Fig. 2. Calculated TSL curves at $T = 4$ K, $E_d = 0.1$ eV, $s = 0.05$, $g_\alpha^2 = 5, \hbar\omega_\alpha = 0.02$ eV, $w_\alpha = 10^{12}$ s^{-1}, $P = 10^{11}$ s^{-1} (*a*); $T = 77$ K, $E_d = 0.25$ eV, $s = 0.07$, $g_\alpha^2 = 10$, $\hbar\omega_\alpha = 0.03$ eV, $w_\alpha = 3 \times 10^{12}$ s^{-1}, $P = 10^{11}$ s^{-1} (*b*)

For estimations we assume that $I_{ji} = 0.001$ eV, $\rho_o = 10^2$ eV^{-1}, $B_\alpha(T) = 1$, $g_\alpha^2 = 0.1$ and obtain $W_\alpha = 10^{11}$ s^{-1}.

In this theoretical section we present the results of calculations using Eqs. (3), (8) for the TSL curve formed by the participation of one or several molecular vibrations of the same α-type at different values of the constant of interaction of charge with vibrations g_α^2 (Fig. 1 and Fig. 2). For small interaction constants constant of molecules with vibrations, the structure appears as a peak of luminescence intensity at a certain temperature, which appears with increasing temperature, and then a sharp dip (Fig. 1). With an increase in the interaction constant g_α^2, additional peaks appear at other temperatures, corresponding to transitions with the absorption of two, three, and more molecular α-type vibrations. For small values of g_α^2, the TSL curve consists of a broad band caused by the

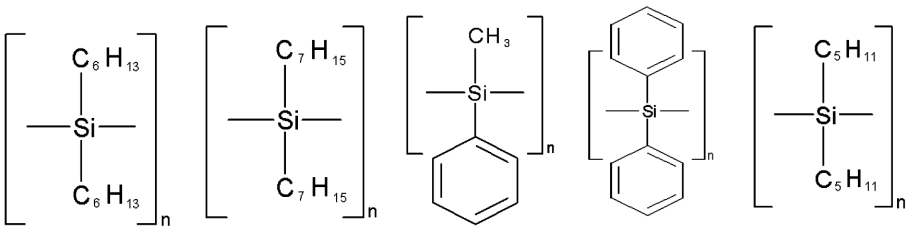

Fig. 3. Structures of silicon organic polymers with differing ordering. The ordering decreases in the figure from left to right

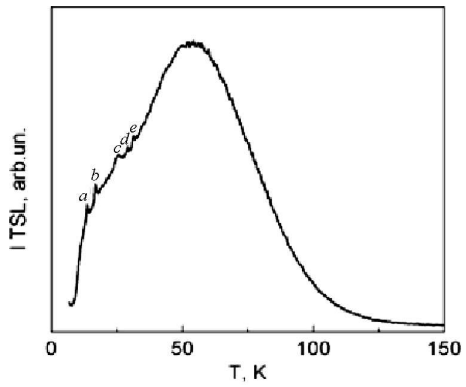

Fig. 4. TSL curve of the PDHS film on a metal substrate

detachment of charges from the traps involving many different vibrations of different types (Fig. 1). For a large interaction constant, the TSL curve has a periodic structure formed by several vibrations of the same type α (Fig. 2). If the quant of vibrational energy is less than the trap depth level energy, a structure on the thermoluminescence curve can appear beginning from an absorption of several vibrational quanta (Fig. 2). Such processes can be observed at higher temperatures, when vibrational levels with higher energies become populated. For example, the structure in Fig. 2, *b* appears upon the absorption of quanta with $m_\alpha > 9$.

3. Experimental Results. Discussions

The silicon organic polymers poly(di-n-hexylsilane) – PDHS, poly(di-n-heptylsilane) – PDHepS, poly(methylphenylsilane) – PMPS, poly(di-n-phenylsilane) – PDPhS and poly(di-n-pentylsilane) – PDPeS polymer films with varying degrees of ordering (Fig. 3) were prepared by direct casting from a toluene solution onto different substrates: metal, sapphire, and quartz.

The details of the preparation of polymer films are described in [18, 19], and nanosized polymer embedded in porous silica is described in [31]. The procedure of the low temperature TSL measurements and the fractional TSL method and regime of the temperature modulation may be found in Refs [14, 15].

3.1. Determination of the TSL curve for PDHS polymer films on different substrates and the activation energies of charge carrier traps

In this section effects of optical vibrations in TSL of PDHS polymers were observed. TSL curves and Raman spectra of the PDHS polymer films deposited on different substrates were measured and the additional structures on TSL curves are analyzed. Activation energies of trapped charge carriers were found by the fractional TSL in the temperature range 5–50 K. The shape of the TSL curve was calculated by the model of Ref. [16], in which the release of carriers from traps can be activated by energy transfer from the vibrations to the carriers. It was found both experimentally and from calculations that the decrease in the degree of polymer ordering causes a decrease of the number of discrete values of activation energies and of the number of the features in TSL curves [18].

It is known that the PDHS films exhibit a significant degree of crystallinity [32]. The degree of the crystallinity of the PDHS polymer reaches 65–80% [33]. Specific ordering in this material is also confirmed by spectroscopic and X-ray data. Indeed, X-ray reflections in PDHS are fairly distinct, and resemble those of a crystalline phase [34–36]. IR [34] and Raman [35, 37–38] spectra of the PDHS consist of narrow bands similar to those observed in crystals.

Figs. 4 and 6 show the integral TSL curves for PDHS films on metal substrate and on sapphire sub-

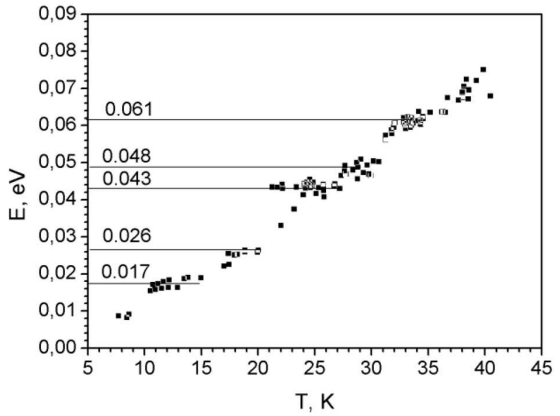

Fig. 5. Activation energies of the traps determined from the fractional TSL for the PDHS film on the metal substrate. The numbers on the horizontal plateaus indicate the activation energies in eV

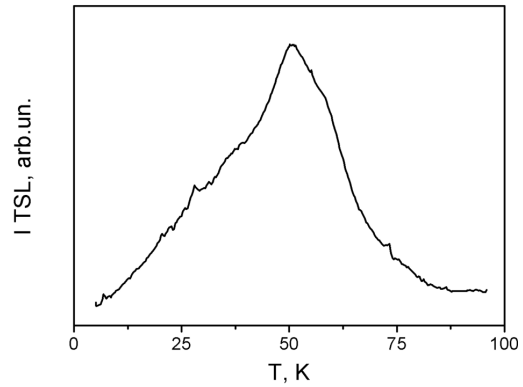

Fig. 6. TSL curve of the PDHS film on the sapphire substrate

strate, respectively, measured for slowly cooled samplest in the 5–150 K temperature range. It should be emphasized that the additional features hereafter referred to as the structure predicted in [16] are clearly observed in these TSL curves. The structure consists of small spikes and dips in the curve and cannot be attributed to noise because it is reproduced in repeated measurements and on different samples.

Figs. 5 and 7 show the activation energies of charge carrier detrapping processes for PDHS films on sapphire substrate measured in the 5–50 K temperature range. The numbers on the horizontal plateaus indicate the activation energies in eV. It is seen that the trap activation energies form six horizontal shelves for the PDHS films: 0.0119 ± 0.0005, 0.0177 ± 0.0003, 0.0263 ± 0.0002, 0.0323 ± 0.0002, 0.0421 ± 0.0003 and 0.0461 ± 0.0005 eV. A comparison of the data obtained

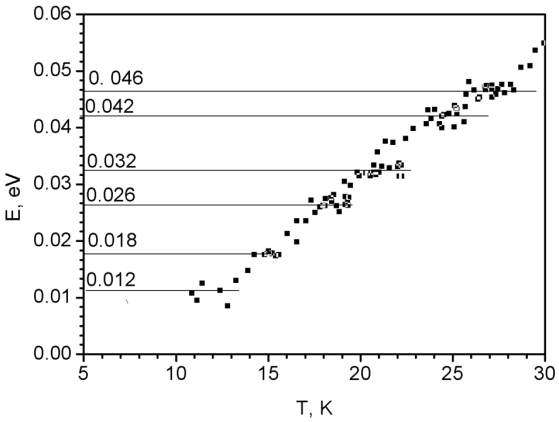

Fig. 7. The activation energies of the traps determined from the fractional TSL for the PDHS film on the sapphire substrate. The numbers on the horizontal plateaus indicate the activation energies in eV

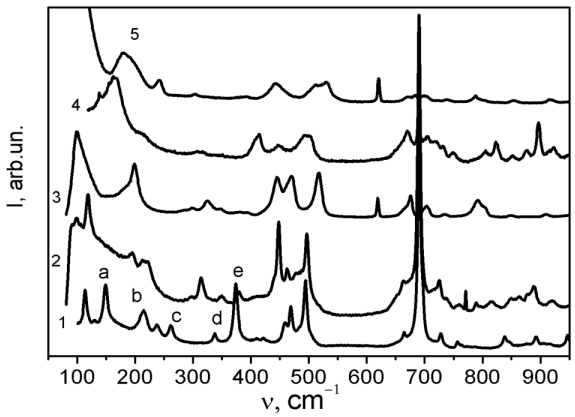

Fig. 8. Raman spectra of polymers PDHS (*1*), PDHepS (*2*) PMPS (*3*), PDPhS (*4*) and PDPeS (*5*) films. The positions of Raman vibrations (*a*–*e*) for PDHS coincide with the activation energy (Fig. 5) and the absorption of these vibrations gives the structure in the TSL curve (Fig. 4)

from the study of TSL (Fig. 7) and Raman spectra (Fig. 8 curve *1*) (see Table 1) showed that the activation energies of the traps correlated well with the frequencies of Si–Si vibrations of the polymer chain: 111 cm^{-1} (0.011 eV), 148 cm^{-1} (0.0183 eV), 214 cm^{-1} (0.0265 eV), 262 cm^{-1} (0.0325 eV), 337 cm^{-1} (0.0418 eV) and 373 cm^{-1} (0.0462 eV), respectively.

The coincidence of activation energies with Raman vibrations and the appearance of the structure in the TSL curves were observed for the PDHS polymer also on metal and quartz substrates too. Summary data are presented in Table 1. Compared with the set of

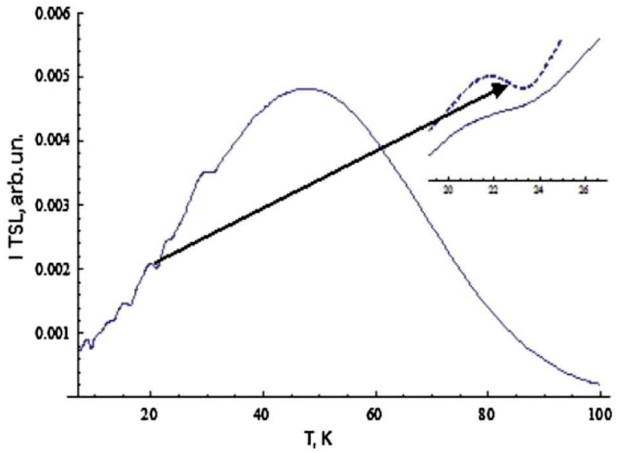

Fig. 9. TSL curve of the PDHS film calculated in [18] for the following parameter values: $E_d = -0.1$ eV, $s = 0.045$ eV for vibrations with energies 0.018 eV, 0.026 eV, 0.032 eV, 0.042 eV, 0.046 eV, 0.061 eV. The inset presents the part of TSL curve in the vicinity of the structure with energy quantum 0.042 eV for different values of the widths of the vibration band: a half-width of 0.001 eV (the dashed line) and 0.003 eV (the continues line)

Table 1. **Comparison of the activation energies of hole traps (E) for the PDHS films on different substrates and the Raman modes of Si–Si vibration in PDHS films [35]. Values in round brackets are given in eV. The bold numbers are given in wavenumber units and the numbers in parentheses are given in electronvolts**

E_{exp}, cm^{-1} (eV)			Raman modes, cm^{-1} (eV)
Sapphir	Metal	Quarts	
97 (0.012)		97 (0.012)	111 (0.011)
143 (0.0177)	137 (0.017)		148 (0.0183)
212 (0.0263)	213 (0.026)	210 (0.026)	214 (0.0265)
260 (0.0323)			262 (0.0325)
339 (0.0421)	344 (0.043)	339 (0.042)	337 (0.0418)
372 (0.0461)	387 (0.048)		373 (0.0462)
	491 (0.061)		493 (0.0611)

activation energies for the PDHS film on the sapphire substrate, in the case of PDHS film on the metal substrate, the values 0.012 and 0.032 eV are missing, but there appears a value of 0.061 eV. Other values are consistent with those obtained for the polymer film on the sapphire substrate.

For the PDHS film on the quartz substrate, three additional peaks on the TSL curve and the activation energies of traps form three horizontal plateaus, which also coincide with the Raman modes of the polymer (Table 1). Repeated TSL measurements revealed a decrease in the observed numbers of both the discrete values of activation energies and the structural features in the TSL curve. This is apparently due to a change in the morphology of the polymer caused by the irradiation. Table 1 shows that the numbers of activation energies for the PDHS polymer depend on the type of substrate and decrease when the substrate is changed from sapphire to metal and quartz.

The same trend is observed for the additional structure in TSL curves of the PDHS polymer. In other words, the observed activation energies for samples on different substrates coincide with the Raman modes, but the number of observed activation energies and additional spikes in the TSL curves on various substrates differs.

We explain these results and the absence of some observed activation energy values for some samples by the sensitivity of the TSL polymer curves to disorder (heterogeneity) of the polymer structure. The heterogeneity leads to the broadening of vibrational bands, and causes a smearing of the features on the TSL curve and reduction in the number of observed discrete levels of the activation energy. The difference in the thermal expansion coefficients between the films and the substrate may cause the change in the structure and the appearance of non-homogeneities in the sample at the polymer cooled to the liquid-helium temperature. The expansion coefficient of quartz differs by an order of magnitude from those of sapphire and metal and by two orders of magnitude from those of the polymer. This may explain the less pronounced additional structure caused by vibrations in the case of the polymer on the quartz substrate (Table 1). However, the results show that the activation energies coincide with the energy quanta of the molecular vibrations. This coincidence is observed for all studied substrates. This supports the model proposed in Ref. [16] of vibration-assisted carrier release from traps. The shape of the TSL curve was calculated in the one-phonon approximation [18] using the model of Ref. [16], under which the release of carriers from traps can be activated by energy transfer from vibrations with different energies: 0.018 eV, 0.026 eV, 0.032 eV, 0.042 eV, 0.046 eV, 0.061 eV to the carriers (Fig. 9). The TSL curve correctly describes

the structure obtained experimentally. It was shown that the number of observed activation energies decreases with increasing widths of optical vibration bands.

These results allow us to conclude that although the trap energy spectrum is quasi-continuous, the release of holes in the polymer is more probable from those, that is localized on traps, the depths of which correspond to the energy of Si–Si vibration of the polymer chain. Another trapped carriers may be released from traps by the simultaneous absorption of several vibrational quanta and thus contribute to the formation of the wide solid TSL curve (Figs. 4, 6). The effects of optical vibrations is more clearly defined in TSL of ordered polymers with low concentration of defects, in which the vibrational bands are narrow.

3.2. Determination of the TSL curve for silicon organic polymer films with varying degrees of ordering and the activation energies of the charge carrier trap

In the present section, the dependence of the charge-carrier release processes in five silicon–organic polymers (PDHS, PDHepS, PMPS, PDPhS, and PDPeS) on their degree of ordering and the widths of vibrational bands is investigated. The study is based on TSL curves, the fractional TSL method in the temperature range of 5–200 K, and Raman spectroscopy. The release of charge carriers from traps via the absorption of vibrational quanta manifests itself both in the appearance of discrete activation energy levels of the carriers, which coincide with the energies of the vibrational quanta, and in the formation of a structured TSL curve. It is shown that the magnitude of these effects depends on the widths of the optical vibrational bands and the degree of polymer ordering. A detailed analysis of all results is presented in [19]; here, only selected data are discussed.

Structures of silicon organic polymers with decreasing ordering are shown in Fig. 3.

It is known that PDHS is a polymer with substantial crystallinity. The other four polymers have a lower degree of ordering relative to PDHS. Compared with the PDHS polymer, the PDPeS is an amorphous polymer. Spectroscopic data indicate that the PDPeS film is in a regular 7/3 helical conformation at room temperature [39]. In comparison to the amorphous

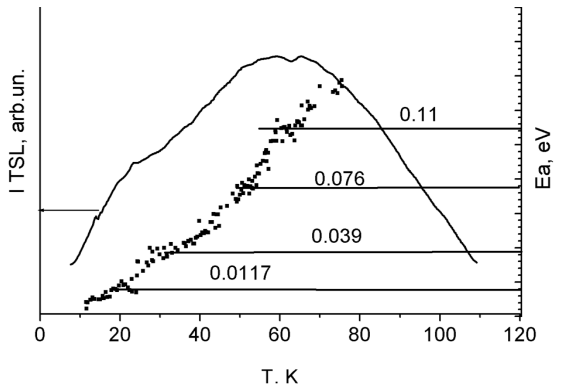

Fig. 10. TSL curve and the activation energies of the PMPS film on the metal substrate

PDPeS film, the PMPS film has 10% crystallinity according to X-ray scattering and the optical polarizing microscopy [40]. Time-resolved fluorescence studies at different temperatures clearly reveal the existence of the ordered conformation in the PMPS film [41].

Fig. 8 shows the measured Raman spectrum of silicon organic polymers with differing degrees of ordering. Raman studies demonstrate that the polymer structure of PMPS and PDPeS films is significantly different from that of the PDHS and these differences are consistent with previously reported data on their structural disorder. First, the bands in the Raman spectra of PMPS and PDPeS are broadened twofold with respect to the bands in the spectrum of PDHS. In particular, the absence of a very intense band at 689 cm^{-1}, which had previously been assigned to a Si–C vibration in the planar zigzag conformation of PDHS, is evident. There are also significant differences in the silicon-silicon stretching region (90–500 cm^{-1}) which indicate that the backbones of PMPS and PDPeS are no longer planar. As will be seen from the subsequent Figs, these polymers have a smaller number of discrete values of activation energies and a less rich structure of TSL curves than for PDHS.

From the analysis of Raman spectra, one may expect the most pronounced effects of the interactions between molecular vibrations and trapped charges in PDHS.

Let us consider how the disordering of polymers and the broadening of their Raman bands affect the manifestation of discrete activation energies.

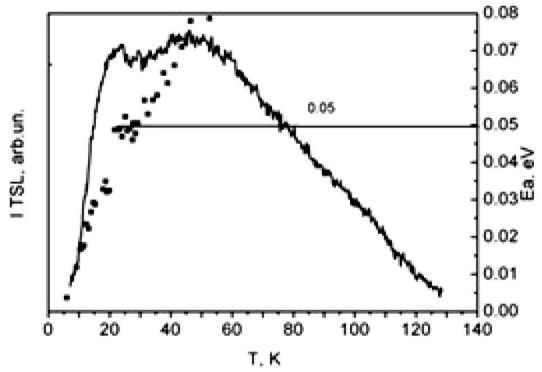

Fig. 11. TSL curve and the activation energies of the PDPeS film on the metal substrate

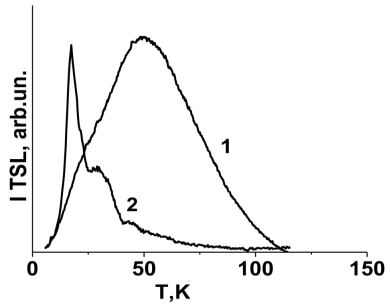

Fig. 12. TSL curve: film of PDHS (*1*) and the nanocomposite PDHS/MCM-41 (*2*). The curves are normalized by the intensity. TSL curves are normalized to the intensity

Table 2. **Comparison of the activation energies of the charge traps (Ea) for silicon organic polymers and the Raman modes of optical vibrations in these polymers. Values of Raman modes in round brackets are given in eV**

PDHS		PMPS		PDPeS	
E_{exp}, cm^{-1} (eV)	Raman modes, cm^{-1} (eV)	E_{exp}, cm^{-1} (eV)	Raman modes, cm^{-1} (eV)	E_{exp}, cm^{-1} (eV)	Raman modes, cm^{-1} (eV)
137 (0.017)	148 (0.0183)	97 (0.0117)	103 (0.0127)	403 (0.05)	414 (0.0513)
211 (0.026)	214 (0.0265)	324 (0.039)	321 (0.0398)		
344 (0.043)	337 (0.0418)	619 (0.076)	615 (0.076)		
370 (0.048)	373 (0.0462)	898 (0.11)	910 (0.12)		
491 (0.061)	493 (0.061)				

Fig. 10 and 11 show the TSL curves of PMPS and PDPeS polymers which have a lower degree of ordering compared to the "crystalline" PDHS polymer (Fig. 6), as well as the activation energy of carrier release from traps in PDHS (Fig. 7) and other polymers. Data on the presence of discrete levels in these polymers and a comparison of their energies with optical vibrational quanta are presented in Table 2.

Some structure is observed in the TSL curve of the PMPS polymer. An essential point for the manifestation of such a structure is the TSL intensity of polymer. Note that the TSL intensities of PMPS and PDHS are almost the same. However, the structure in the TSL curve of PMPS is less pronounced than that observed in PDHS. It can be explained by the broader optical width of the Raman vibrations in PMPS than in PDHS.

Table 2 shows that the activation energies for all polymers coincide with the energies of the quanta of molecular vibrations. The appearance of a structure in the TSL curve is also observed. However, it follows from Table 2 that the number of observed activation energies and features in the additional structure in TSL curves (Figs. 10, 11) are less than that of the PDHS polymer (Fig. 7). This is due to the fact that the number of observed activation energies decreases with the increase of widths of optical vibration bands and with the decrease of ordering of polymers.

Thus, the manifestation of optical vibrations in the processes of carrier release from traps is more pronounced in TSL of ordered silicon organic polymers with low concentration of defects, in which the vibrations bands are narrow, and the intensity of the TSL is significant. The heterogeneity leads to the broadening of vibration bands and causes a reduction in the number of observed discrete activation energy levels of traps in silicon organic polymers. The same processes have also been observed in studies of TSL polygermane polymers [42].

3.3. Experimental study of low-temperature TSL of the PDHS/MCM-41 nanocomposite

In this section an experimental and theoretical study of the TSL of the PDHS/MCM-41 nanocomposite obtained by the introduction the PDHS polymer into MCM-41 nanopores with a pore diameter of 2.8 nm was carried out in the temperature range of 5–120 K [31]. A significant role of molecular vibrations in the formation of the TSL curves is observed.

Fig. 12 shows the TSL curves of the PDHS polymer film and the PDHS/MCM-41 nanocomposite. It should be noted that the intensity of the nanocomposite curve is significantly lower than that of the polymer film. The TSL curve of PDHS/MCM-41 nanocomposite consists of two bands: a very narrow and intense band at 16 K with a half-width of 8 K, and a weaker, broader band with a maximum at 31 K. It is shown that the TSL curve of the nanocomposite is shifted toward lower temperatures by 34 K compared with that of the polymer film, while its half width is reduced by a factor of 6 and its shape is changed.

Since there is only one polymer chain in the pores of MCM-41, the number of traps in this case is significantly smaller than in the polymer. This is associated with a shift of the maximum of the TSL curve of the PDHS/MCM-41 nanocomposite towards low temperatures by 32 K and to a narrowing of its half-width relative to the half-width of the TSL curve of the film by 6 times. The orientation of the polymer chain in the MCM-41 pore also leads to a decrease in the concentration of defects in the polymer chain, which also contributes to the narrowing of the half-width of the TSL curve of the PDHS/MCM-41 nanocomposite.

Fig. 13 shows the temperature dependence of the trap activation energy of the PDHS/MCM-41 nanocomposite. It can be seen that the trap activation energy forms only two horizontal plateaus: 0.032 and 0.046 eV. We emphasize that these activation energies correspond to the more intense polymer vibrational modes at 262 см^{-1} and to the fully symmetrical vibration at 373 см^{-1}, respectively. Note that, in contrast, the trap activation energy of the PDHS film forms six horizontal shelves (Fig. 7).

Thus, it was shown that the positions of the activation energies are discrete and they coincide with the energies of Si–Si vibration of the polymer. The TSL curve was calculated using Eq. (3) and taking into account relations (9)–(11). The parameters were chosen in such a way that the calculated curve $I(T)$ described the experimental curve *2* in Fig. 12. The calculations took into account two molecular vibrations observed in Fig. 13 with quantum energies for $\alpha = 1$ ($E_1 = 0.046$ eV (373 см^{-1})) and for $\alpha = 2$ ($E_2 = 0.032$ eV (262 см^{-1})).

(The experimentally observed decrease in the number of vibrational modes from six to two for molecules in a pore is possibly due to the inhibition of transverse molecular motions by the pore walls.)

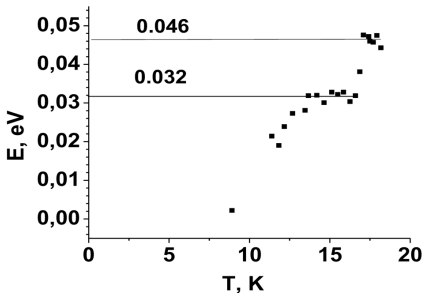

Fig. 13. Activation energies of the traps for the PDHS/MCM-41 nanocomposite. The numbers on the horizontal plateaus indicate the activation energies in eV

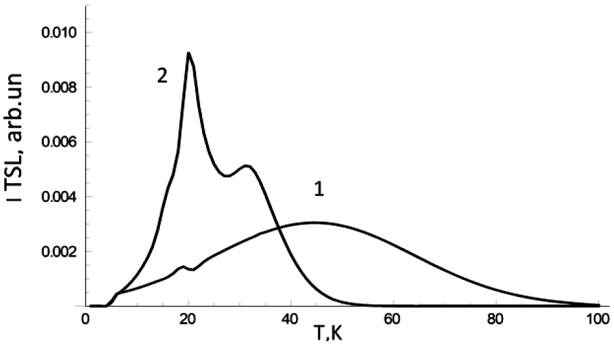

Fig. 14. Temperature dependence of the TSL intensity for a polymer film (curve *1*) and polymer molecules confined in a pore (curve *2*). The calculations were carried out for the same numbers of carriers created by light in the film and in the pores. Curve parameters: for the polymer in the pore: $s = 0.02$ eV, $E_d = 0.06$ eV, $s_l = 0.001$ eV, $W_1 = 10^{11}$ s^{-1}, $W_2 = 5 \times 10^9$ s^{-1}, $P = 2 \times 10^{10}$ s^{-1}, for the film $s = 0.05$ eV, $E_d = 0.11$ eV, $s_l = 0.0005$ eV, $W_1 = 10^{11}$ s^{-1}, $W_2 = 5 \times \times 10^9$ s^{-1}, $P = 10^{11}$ s^{-1}

The model of description and results of calculations presented in Fig. 14 correctly describe the experiment presented in Fig. 12. The different ratios of TSL intensity maxima in the film and in the pores in Figs. 12 and 14 are due to the fact that in Fig. 12 the maxima are normalized to the same reference intensity.

Naturally, experimental measurements for film and nanocomposites were performed on different samples. The calculations, carried out for the same number of molecules in both cases, allow us to compare the band intensities and show a decrease in the intensity of the broad band consistent with the experiment.

The TSL curve of the polymer in the pores and the polymer film are significantly different. As one would expect, the shift and the width of the energy spectrum for a polymer in a pore is narrower than in the

film. The shift in pore is equal to $s = 0.02$ eV, while for a film $s = 0.05$ eV [16–19]. The probabilities of multiphonon processes also differ greatly in the film and in the pore. The role of multiphonon processes in the pore decreases since the number of vibrations in a pore is less rich due to a decrease in the number of neighbors. The narrow peak in the TSL curve in Fig. 14 at $T \sim 20$ K is due to the molecular vibration with $E_1 = 0.046$ eV. Vibration with $E_1 = 0.032$ eV is not observed experimentally. This indicates that the probability to transfer the charger from a trap via the absorption of a single quant of this vibration is less than a critical value. This vibration and all other vibrations form in pore the band with a lower intensity maximum in Fig. 14 at $T \sim 35$ K and broad band (curve *1* in Fig. 12 and in Fig. 14) in a bulk sample.

Thus, from experimental data (Fig. 12) and from the calculations (Fig. 14) it follows that for a polymer molecule in a pore, the role of individual molecular vibrations increases in processes of TSL. The vibration manifests itself as a sharp peak in the TSL curve. At the same time, in bulk samples, processes with the absorption of individual vibrations, observed in [16–19] (Figs. 4, 6, 10, 11) and in the curve *1* of Fig. 14, appear in the form of small features on the TSL curve.

4. Conclusion

This paper analyzes TSL features arising from the participation of individual molecular vibrations of polymers in the processes of detachment of a localized charge from a trap. Taking these processes into account is important for the following reasons.

1) Traditional methods for determining the activation energy of traps in polymers, such as those obtained by the widely used fractional TSL method, can lead to incorrect results. Despite the quasi-continuous nature of the energy spectrum of traps in polymers, molecular vibrations lead to the appearance of discrete activation levels with a depth equal to the vibrational quantum energy. These features should be taken into account when analyzing and drawing conclusions from experiments about spectrum of charge traps.

2) The magnitude and nature of structural features on the TSL curve caused by molecular vibrations provide information about the investigated systems and about the strengths of the electron-vibrational interactions for individual vibrations.

3) Similar manifestations of molecular vibrations may also occur in other processes, for example, in the temperature dependence of the electrical conductivity of polymers.

The authors thank Dr. A.F. Gumenyuk for the help in the study of TSL polymers, Prof. Liviu Sacarescu for providing the PDPhS polymer, Prof. Akira Watanabe for providing other polymers.

1. E.A. Tikhonov, M.T. Shpak. *Nonlinear Optical Phenomena in Organic Compounds* (Naukova Dumka, 1988).
2. N.I. Ostapenko, V.I. Sugakov, M.T. Shpak. *Spectroscopy of Defects in Organic Crystals* (Kluwer Academic Publishers, 1993).
3. E.N. Velikaya, A.K. Kadashchuk, N.I. Ostapenko, Yu.A. Skryshevsky, M.T. Shpak. Tunneling and thermally activated processes in polymers. *Sov. Phys. Solid State* **31**, 203 (1989).
4. R.A. Partridge. Electron traps in polyethylene. *J. Polym. Sci. A* **2817**, 10003080 (1965).
5. V.G. Nikolskii, G.I Burkov. Radiothermoluminescence of some polymers irradiated at 77 K. *High Energy Chem.* **5**, 373 (1971).
6. D. Ito, T. Nakahita. Thermally stimulated current and thermoluminescence due to electron detrapping by local molecular motions in polyethylene-terephthalate. *J. Appl. Phys.* **51**, 3273 (1980).
7. J. Vanderschueren, A. Linkens, J. Niezette. Effect of doping on thermoluminescence in of activation energy polymers. I. 9,10-phenanthrenequinone-doped polydiancarbonate. *J. Polym. Sci. B* **24**, 697 (1986).
8. R.J. Fleming, J. Hagekyriakou. Thermoluminescence in polymers. *Radiat. Prot. Dosim.* **8**, 99 (1984).
9. L Zlatkevich. *Radiothermoluminescence and Transitions in Polymers* (Spinger-Verlag, 1989).
10. E. Dobruchowskaa, L. Okrasaa, I. Glowackia, J. Ulanski, G. Boiteux. The wet dog' effect in polymers as seen by thermoluminescence. *Polymer* **45**, 6027 (2004).
11. D.V. Lebedev, E.N. Vlasova, E.M. Ivan'kova, A.A. Kalachev, V.A. Marikhin, L.P. Myasnikova, A.V. Naschekin, E.I. Radovanova. Possibilities of thermoluminescence method for estimating the molecular packing in near-surface layers of polymers. *J. Struct. Chem.* **51**, 116 (2010).
12. I.S. Gorban, A.F. Gumenyuk, V.A. Omel'yanenko. Thermoluminescence and polaron states in barium-sodium niobate crystals. *Ukr. Fiz. Zh.* **33**, 530 (1988) (in Russian).
13. O. Stanovyi, S. Kutovyy, A. Gumenyuk, I. Dmitruk. Polaron model of traps and their activation energies in KBr crystals. *Nano-Electron. Phys.* **9**, 04009 (2017).
14. A. Gumenyuk N. Ostapenko, Yu. Ostapenko, O. Kerita, S. Suto. Unusual features of charge carrier traps energy

spectra in silicon organic polymers revealed by enhanced TSL. *Chem. Phys.* **394**, 36 (2011).

15. A. Gumenjuk N. Ostapenko, Yu. Ostapenko, O. Kerita, S. Suto. Oscillatory regularity of charge carrier traps energy spectra in silicon organic polymer poly(di-n-hexylsilane). *Low Temp. Phys.* **38**, 932 (2012).
16. V.I. Sugakov, N.I. Ostapenko. Effect of molecular optical vibrations on thermoluminescence of silicon organic polymer. *Chem. Phys.* **456**, 22 (2015).
17. V. Sugakov, N. Ostapenko, Yu. Ostapenko, O. Kerita, V. Strelchuk, O. Kolomys, A. Watanabe. Interaction of optical vibration with charge traps and the thermoluminescence spectra of polymers, *Ukr. J. Phys.* **61**, 531 (2016).
18. V. Sugakov, N. Ostapenko, Yu. Ostapenko, O. Kerita, V. Strelchuk, O. Kolomys. Molecular vibrations, activation energies of trapped carriers and additional structure in thermoluminescence of organic polymers. *Synth. Met.* **234**, 117 (2017).
19. V. Sugakov, N. Ostapenko, Yu. Ostapenko, O. Kerita, V. Strelchuk, O. Kolomys. Experimental and modeling study of charge carriers release from traps by interaction with molecular vibrations in silicon organic polymers. *Mol. Cryst. Liq. Cryst.* **697**, 68 (2020).
20. A. Miller, E. Abrahams. Impurity conduction at low concentrations. *Phys. Rev.* **120**, 745 (1960).
21. H. Bässler. Charge transport in disordered organic photoconductors. Monte Carlo simulation study. *Phys. Status Solidi B* **175**, 15 (1993).
22. V.I. Arkhipov, E.V. Emilianova, A. Kadashchuk, H. Bässler. Thermally stimulated photoluminescence in disordered organic materials. *Chem. Phys.* **266**, 97 (2001).
23. S.D. Baranovskii. Theoretical description of charge transport in disordered organic semiconductors. *Phys. Status Solidi* **251**, 487 (2014).
24. V.I. Sugakov. Fine structure of thermoluminescence assisted by molecular vibrations in disordered organic semiconductors. *J. Phys.: Condens. Matter.* **34**, 185703 (2022).
25. S.I. Pekar. On the theory of luminescence and light absorption by impurities in dielectrics. *Sov. Phys. JETP* **22**, 641 (1952).
26. M.D. Frank-Kamenetskii, A.V. Lukashin. Electron-vibrational interactions in polyatomic molecules. *Sov. Phys. Usp.* **18**, 391 (1975).
27. J. Jortner. Temperature dependent activation energy for electron transfer between biological molecules. *J. Chem. Phys.* **54**, 4860 (1976).
28. V. Stern, R.F. Fink, M. Tafipolski, C. Deibel, B. Engels. Comparison of different rate constant expressions for the prediction of charge and energy transport in oligoacenes. *WIREs Comput. Mol. Sci.* **6**, 694 (2016).
29. X. de Vries, P. Friederich, W. Wenzel, R. Coehoorn, P.A. Bobbert. Full quantum treatment of charge dynamics in amorphous molecular semiconductors. *Phys. Rev. B* **97**, 075203 (2018).
30. R.A. Marcus. Electron transfer reactions in chemistry. Theory and experiment. *Rev. Mod. Phys.* **65**, 599 (1993).
31. N.I. Ostapenko, Yu.V. Ostapenko, V.I. Sugakov. Manifestation of molecular vibrations of polymers in thermoluminescence of nanocomposites. *Mol. Cryst. Liq. Cryst.* **768**, 788 (2024).
32. M. Pope, C.E. Swenberg. *Electronic Processes in Organic Crystals and Polymers* (Oxford University Press, 1999).
33. M.M. Despotopoulou, R.D. Miller, J.F. Rabolt, C.W. Frank. Polymer chain organization and orientation in ultrathin films: A spectroscopic Investigation. *J. Polym. Sci. B* **34**, 2335 (1996).
34. J.F. Rabolt, D. Hofer, R.D. Miller, G.N. Fickes. Studies of chain conformational kinetics in poly(di-n-alkylsilanes) by spectroscopic methods. 1. Poly(di-n-hexylsilane), poly(di-n-heptylsilane), and poly(di-n-octylsilane). *Macromolecules* **19**, 611 (1986).
35. H. Kuzmany, J.F. Rabolt, B.L. Farmer, R.D. Miller. Studies of chain conformational kinetics in poly (di-n-alkylsilanes) by spectroscopic methods 2. Conformation and packing of poly (di-n-hexylsilane). *J. Chem. Phys.* **85**, 7413 (1986).
36. C.A. van Walree, T.J. Cleij, L.W. Jenneskens, G.P. van der Laan, M.P. de Haas, E.T.G. Lutz. Structural, photophysical, and conductive properties of n-hexyl substituted hybrid polysilylene–polysilyne networks. *Macromolecules* **29**, 7362 (1996).
37. S.S. Bukalov, L.A. Leites, G.I. Magdanurov, R. West. Low-temperature Raman spectra and the structure of some permethylpolysilanes. *J. Organomet. Chem.* **521**, 107 (1996).
38. L.A. Leites, S.S. Bukalov, T.S. Yadritzeva, M.K. Mokhov, B.A. Antipova, T.M. Frunze, V.V. Dement'ev. Vibrational and electronic spectra and the structure of crystalline poly(dimethylsi1ane). *Macromolecules* **25**, 2991 (1992).
39. R.D. Miller, B.L. Farmer, W. Fleming, R. Sooriyakumaran, J.F. Rabolt. Poly(di-n-pentylsilane): the spectral consequences of a disordered backbone conformation. *J. Am. Chem. Soc.* **109**, 2509 (1987).
40. S. Demoustier-Champagne, A. Jonas, A. Devaux. Poly(methylphenyl) silane: structural properties. *J. Polym. Sci. B* **35**, 1727 (1997).
41. N. Ostapenko, V. Gulbinas, R. Augulis, A. Boiko, M. Chursanova, A. Volkov, G. Telbiz. Fluorescence relaxation kinetics of poly(methylphenylsilane) film and nanocomposites. *Nanosc. Res. Lett.* **11**, 1 (2016).
42. N.I. Ostapenko, O.A. Kerita, Yu.V. Ostapenko, M.V. Chursanova. Effect of the polymer ordering on the optical spectra and thermoluminescence of polygermane and polysilane films and nanocomposites. *Low Temp. Phys.* **45**, 748 (2019).

Received 25.12.25

Н.І. Остапенко, В.Й. Сугаков

ОСОБЛИВОСТІ ВПЛИВУ
МОЛЕКУЛЯРНИХ КОЛИВАНЬ
НА ТЕРМОЛЮМІНЕСЦЕНЦІЮ ПОЛІМЕРІВ

У статті представлено результати спостереження й дослідження проявів окремих молекулярних коливань у процесах термолюмінесценції полімерів. Ці прояви мають такі особливості: 1) попри квазинеперервний спектр енергій пасток для носіїв заряду в полімерах, енергії активації, визначені методом фракційної термолюмінесценції, мають дискретні значення; 2) ці значення енергій активації збігаються з квантами молекулярних коливань у системі; 3) температурна залежність інтенсивності термолюмінесценції має характерну поведінку, зумовлену молекулярними коливаннями. Таку температурну залежність і енергії активації було експериментально досліджено для полімерів, нанесених на різні підкладинки, полімерів з різним ступенем кристалічності та нанорозмірних полімерів, вбудованих у пористий кремнезем. Експериментальні результати узгоджуються з запропонованою моделлю участі молекулярних коливань у процесах вивільнення заряду з пасток під час термолюмінесценції.

Ключові слова: термолюмінесценція, полімерні плівки, нанокомпозит, молекулярні коливання, енергії активації.